International Journal for Innovative Engineering and Management Research
A Peer Revieved Open Access International Journal
www.ijiemr.org

COPY RIGHT

IJIEMR Transactions, online available on 19th June 2017. Link :
http://www.ijiemr.org/downloads.php?vol=Volume-6&issue=ISSUE-4

Title: Pv Cell Fed Hybrid Boosting Converter For Induction Motor Drive Applications.

Volume 06, Issue 04,Page No: 1130 – 1140.

Paper Authors

*** SHAIK P K JAMEERHUSSAIN, **R RAGHUNATH SASTRY.**
* Dept EEE, NRI Engineering College, Agiripalli, Krishna (Dt).

USE THIS BARCODE TO ACCESS YOUR ONLINE PAPER

To Secure Your Paper As Per UGC Guidelines We Are Providing A Electronic Bar Code

International Journal for Innovative Engineering and Management Research
A Peer Revieved Open Access International Journal
www.ijiemr.org

PV CELL FED HYBRID BOOSTING CONVERTER FOR INDUCTION MOTOR DRIVE APPLICATIONS

***SHAIK P K JAMEERHUSSAIN, **R RAGHUNATH SASTRY**

PG Scholar, Dept EEE, NRI Engineering College, Agiripalli, Krishna (Dt); A.P, India.

Associate Professor, Dept EEE, NRI Engineering College, Agiripalli, Krishna (Dt); A.P, India.

ABSTRACT:

A suitable DC-DC converter is required for designing high efficiency power systems. Among the various topologies, Hybrid Boost converter (HBC) is considered as a better solution for high power systems due to improved electrical performance, reduced weight and size. Detailed analysis has been done to investigate the benefits of multi device interleaved boost converter compared to the conventional boost converter topologies. Hybrid Boost converter (HBC) is proposed for high-voltage and high-power applications. One of challenge in designing a boost converter for high power application is how to handle the high current at the input side. A multi device structure with interleaved control is proposed to reduce the input current ripples, the output voltage ripples, size and weight of the passive components with high efficiency compared with the other topologies. By virtue of the converters, the input current can be shared among the cells or phases, so that high reliability and efficiency in power electronic systems can be obtained. In addition, it is possible to improve the system characteristics such as maintenance, repair, fault tolerance, and low heat dissipation. Moreover, the overall performance of the compromised design was shown to be quite good. In addition, low EMI and low stress in the switches are expected, which decreases the conduction losses and lengthens the life time of input source. Even the low voltage stress makes the low-voltage rated switching devices can be adopted for reductions of conduction losses and cost. The developed hybrid boost converter steps up the voltage produced by the PV array to a value which is suitable to run an induction motor.By using a LC filter pure sine wave is obtained which can be directly used to drive a induction motor drive application.

Key words: PV System, Hybrid Boost Converter, Induction Motor.

1. INTRODUCTION

In general, manufacturers provide 5 second and ½ an hour surge figures which give an indication of how much power is supplied by the inverter. Solar inverters require a high efficiency rating. Since use of solar cells remains relatively costly, it is paramount to adopt high efficiency inverter to optimize the performance of solar energy system. High reliability helps keep maintenance cost low.

Since most solar power stations are built in rural areas without any monitoring manpower, it requires that inverters have competent circuit structure, strict selection of components and protective functions such as internal short circuit protection, overheating protection and overcharge protection. Wider tolerance to DC input current plays an important role, since the terminal voltage varies depending on the load and sunlight [1-4]. Though energy storage

International Journal for Innovative Engineering and Management Research
A Peer Revieved Open Access International Journal
www.ijiemr.org

batteries are significant in providing consistent power supply, variation in voltage increases as the battery's remaining capacity and internal resistance condition changes especially when the battery is ageing, widening its terminal voltage variation range. In midto-large capacity solar energy systems, inverters' power output should be in the form of sine waves which attain less distortion in energy transmission. Many solar energy power stations are equipped with gadgets that require higher quality of electricity grid which, when connected to the solar systems, requires sine waves to avoid electric harmonic pollution from the public power supply. [5]

How Inverters Work: There are three major functions an inverter provides to ensure the operation of a solar system one of the most efficient and promising way to solve this problem is the use of pumping and water treatment systems supplied by photovoltaic (PV) solar energy. Such systems aren't new, and are already used for more than three decades [6-8]. But until recently the majority of the available commercial converters are based on an intermediate storage system performed with the use of batteries or DC motors to drive the water pump. The batteries allow the system to always operate at its rated power even in temporary conditions of low solar radiation [9-10]. This facilitates the coupling of the electric dynamics of the solar panel and the motor used for pumping. Generally, batteries used in this type of system have a low life span, only two years on average, which is extremely low compared to useful life of 15 years of a photovoltaic module. Also, they make the cost of installation and maintenance of such systems substantially high. Furthermore, the lack of batteries replacement is responsible for total failure of such systems in isolated areas this type of system normally uses low-voltage DC motors, thus avoiding a boost stage between the PV module and the motor [11]. Unfortunately, DC motors have low efficiency and high maintenance cost and is not suitable. For such applications the use of a three phase induction motor, due to its high degree of robustness, low cost, higher efficiency and lower maintenance cost compared to other types of motors. These requirements make necessary use of a converter with features high efficiency; low cost; autonomous operation; robustness and high life span [12-13].

II. PROPOSED GENERAL HBC TOPOLOGY AND ITS OPERATIONAL PRINCIPAL

The proposed HBC is shown in Fig. 1. There are two versions of HBC, odd-order HBC and even-order HBC as shown in Fig.1 (a) and (b). The even-order topology integrates the input source as part of the output voltage, leading to a higher components utilization rate with respect to the same voltage gain. However, they share similar other characteristics andcircuit analysis method. Therefore, only even-order topology is investigated in this paper.

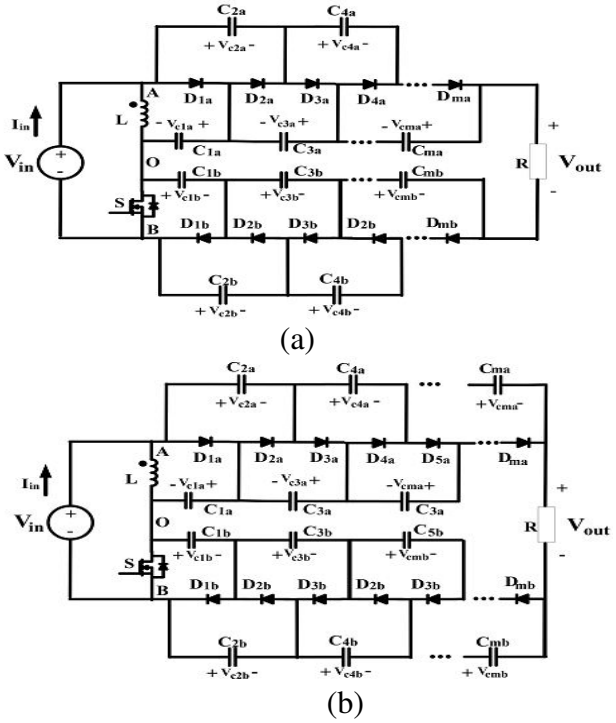

Fig.1. Proposed general HBC topology. (a) Odd-order HBC. (b) Even-order HBC.

International Journal for Innovative Engineering and Management Research
A Peer Revieved Open Access International Journal
www.ijiemr.org

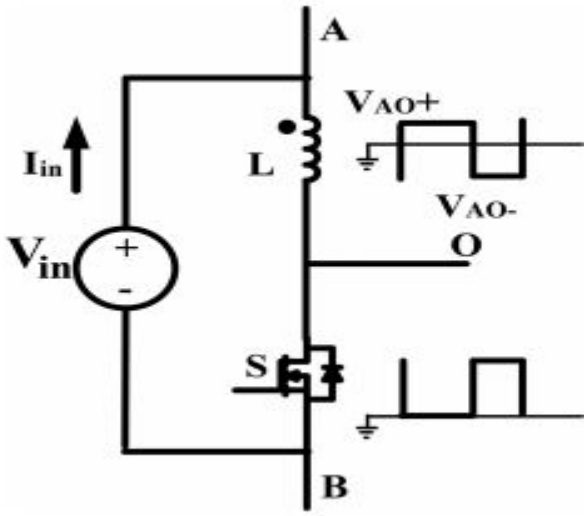

Fig.2. Inductive three-terminal switching core

A. Inductive Switching Core

In a HBC topology, the inductor, switch and input source serve as an "inductive switching core," shown as Fig. 2. It can generate two "complimentary" PWM voltage waveforms at port AO and port OB. Although the two voltage waveforms have their individual high voltage level and low voltage level, the gap between two levels is identical, which is an important characteristic of inductive switching core for interleaving operation.B. BVM

A BVM is composed of a positive multiplier branch and a negative multiplier branch, shown in Fig. 3(a) and (b). Positive multiplier is the same as traditional voltage multiplier while the negative multiplier has the input at the cathode terminal of cascaded diodes, which can generate negative voltage at anode terminal, shown in Fig.3 (b). By defining the high voltage level at input AO as VOA+, the low voltage level as VOA−, and the duty cycle of high voltage level as D, the operational states of the even-order positive multiplier is derived as Fig. 5 and illustrated as following:

1) State 1[0, DTs]: When the voltage at port AO is at high level, diodes Dia (i=2k−1, 2k−3...3, 1) will be conducted consecutively. Each diode becomes reversely biased before the next diode fully conducts. There are K sub states resulted as shown in Fig. 4(a). Capacitor Cia (i=2, 4...2k) are discharged during this time interval. Assuming the flying capacitors get fully charged at steady state and diodes voltage drop are neglected, the following relationship can be derived:

$$V_{c1a} = V_{AO+} \quad (1)$$

$$V_{cia} = V_{c(i+1)a}(i = 2,4,6,\ldots,2k-2) \quad (2)$$

2) State 2[dTs, Ts]: When the voltage at port AO steps to low level, diode D2ka is conducted first, shown as Fig.3(b)-(1). Then the diodes Dia (i=2, 4, ... 2k−2) will be turned on one after another from high number to low. Each diode will be turned on when the previous one becomes blocked. Only diode D2ka is conducted for the whole time interval of [0, dTs], since capacitor C (2k−1) a has to partially provide the

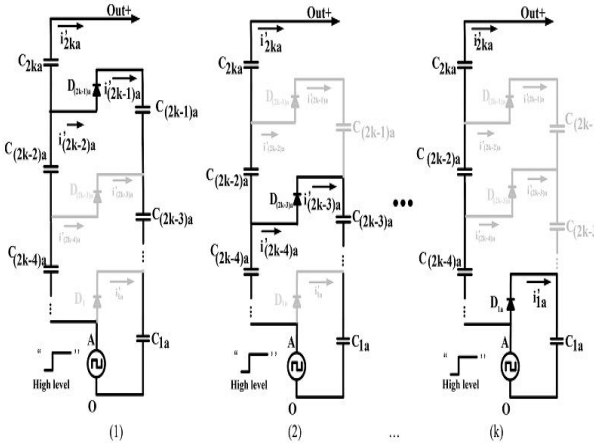

(a)

Fig.3. Operation modes of even-order BVM positive branch (a) State 1[0, DTs]. (b) State 2[DTs, Ts]

Load current during the whole time interval. Even though not all the diodes are conducted and blocked at the same time, the flying capacitors still have the following relationship by the end of this time interval:

$$V_{c2a} = V_{c1a} - V_{AO-} \quad (3)$$

International Journal for Innovative Engineering and Management Research
A Peer Revieved Open Access International Journal
www.ijiemr.org

$$V_{cia} = V_{c(i+1)a}(i = 3,5,7,\ldots,2k-1) \quad (4)$$

According to charge balance principal, the total amount of electrical charge flowing into capacitors Cia (i=2, 4, 2k) should equal to that coming out from them in a switching period at steady state, therefore

$$\sum_{i=1}^{k}\int_{0}^{DT_S} i'_{2ia}\,dt = \sum_{i=1}^{k}\int_{DT_S}^{T_S} i_{2ia}\,dt \quad (5)$$

Thus, the capacitor group Cia (i=2, 4...2k) can be replaced by an equivalent capacitor C2a (eq).The diode group Dia (i=2, 4...2k) which provides the charging path for C2a (eq) is equivalent to a single diode C2a (eq). Similarly, the capacitor group Cia (i=1,3, ... 2k−1) can be replaced by an equivalent capacitor C1a(eq) and diode group Dia (i= 1,3, ... 2k−1)byD1a (eq) . The final equivalent even-order positive multiplier branch is given as Fig.4 (a). A similar analysis yields the equivalent negative multiplier branch as shown in Fig.4 (b). According to (1)–(4), the voltage of equivalent capacitors C1a (eq), C2a (eq) can be expressed as following:

$$V_{c2a(eq)} = k(V_{AO+} - V_{AO-}) \quad (6)$$

$$V_{c1a(eq)} = (k-1)(V_{AO+} - V_{AO-}) + V_{AO+} \quad (7)$$

For the negative branch shown in Fig.4 (b), the following results can be obtained based on similar analysis:

$$V_{c2b(eq)} = k(V_{OB+} - V_{OB-}) \quad (8)$$

$$V_{c1b(eq)} = (k-1)(V_{OB+} - V_{OB-}) + V_{OB+} \quad (9)$$

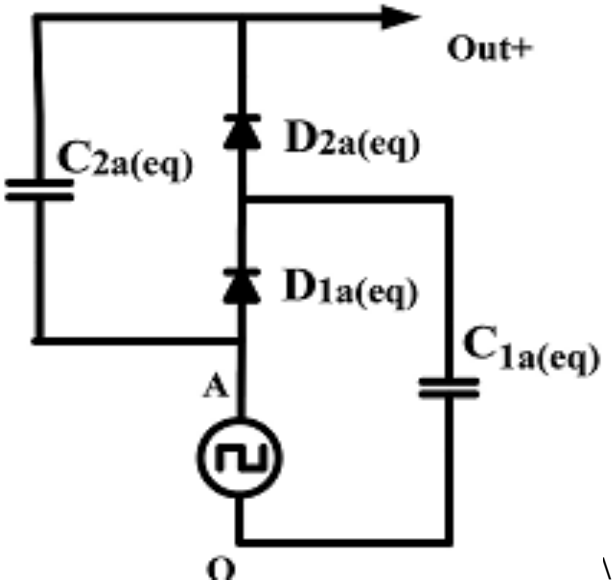

(a)

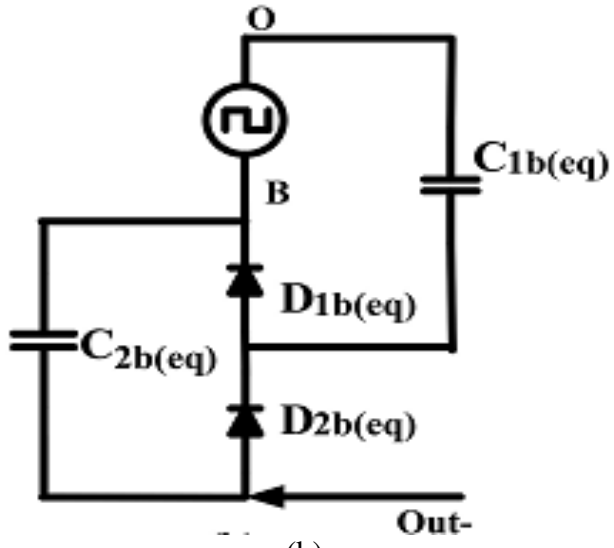

(b)

Fig.4.Equivalent circuit (a) Even-order positive multiplier. (b) Even-order negative multiplier Where $V_{OB}+$ is the high voltage level of input port OB and $V_{OB}-$ is the low voltage level.

2) Equivalent Capacitance Derivation: Assuming capacitors Cia (i=1, 2, 3, ... 2k) have the same capacitance C, in order to derive the equivalent capacitance of C2a (eq) and C1a (eq) in expression of C, a voltage ripple-based calculation method is proposed in this section. Assuming the peak to peak voltage ripple of the

International Journal for Innovative Engineering and Management Research
A Peer Revieved Open Access International Journal
www.ijiemr.org

3) flying capacitors can be expressed as ΔVcia (i=1, 2, 3...2k), the ripple of equivalent capacitor C2a (eq) is ΔV, the following relationship can be approximated:

$$\Delta V = \Delta V_{c2a} + \Delta V_{c4a} + \dots \Delta V_{c2ka} \quad (10)$$

$$\overline{i'_{ia(\text{on})}} DT_S = \overline{i_{ia(\text{off})}} D'T_S (i = 2, 4, \dots 2k) \quad (11)$$

At the same time, state 1 gives

$$\overline{i'_{ia(\text{on})}} = \overline{i'_{(i+1)a(\text{on})}} (i = 2, 4, \dots 2k-2) \quad (12)$$

State 2 gives

$$\overline{i_{ia(\text{off})}} = \overline{i_{(i+1)a(\text{off})}} (i = 1, 3, \dots 2k-3) \quad (13)$$

Based on the (11)–(13), the following relationship can be obtained:

$$\overline{i_{2a(\text{off})}} = \overline{i_{4a(\text{off})}} = \dots \overline{i_{(2k-4)a(\text{off})}} = \overline{i_{(2k-2)a(\text{off})}} = \overline{i_{(2k-1)a(\text{off})}} \quad (14)$$

Based on charge balance of capacitor C2ka, it can be derived that

$$\overline{i_{2(k-1)a(\text{off})}} D'T_S = I_O T_S \quad (15)$$

$$\overline{i_{2ka(\text{off})}} D'T_S = \overline{i'_{2ka(\text{on})}} DT_S = I_O DT_S \quad (16)$$

Where

$$I_o = \frac{V_{\text{out}}}{R}.$$

According to KCL in Fig.3 (b), voltage ripple of capacitors Cia (i=2, 4...2k) can be obtained

$$\begin{cases} C\Delta V_{c2a} = (\overline{i_{2ka(\text{off})}} + \overline{i_{2k-2a(\text{off})}} + \dots \overline{i_{4a(\text{off})}} + \overline{i_{2a(\text{off})}}) D'T_S \\ C\Delta V_{c4a} = (\overline{i_{2ka(\text{off})}} + \overline{i_{2k-2a(\text{off})}} + \dots \overline{i_{4a(\text{off})}}) D'T_S \\ \dots \\ C\Delta V_{c2ka} = \overline{i_{2ka(\text{off})}} D'T_S \end{cases} \quad (17)$$

Where

$$D' = 1 - D$$

Based on the equations from (14) to (16), the equation group (17) can be reduced to the following expression:

$$\begin{cases} C\Delta V_{c2a} = (k - 1 + D) I_O T_S \\ C\Delta V_{c4a} = (k - 2 + D) I_O T_S \\ \dots \\ C\Delta V_{c2ka} = (0 + D) I_O T_S \end{cases} \quad (18)$$

Substituting (10) to (18), the following equation is derived:

$$C\Delta V = \left(\frac{k(k-1)}{2} + kD \right) I_O T_S \quad (19)$$

Meanwhile, the following equation can be derived based on discharging stage of equivalent capacitor C2a (eq)

$$C_{2a(eq)} \Delta V = I_O DT_S \quad (20)$$

Based on (19) and (20), the equivalent capacitor C2a (eq) can be expressed

$$C_{2a(eq)} = \frac{2D}{k(k-1+2D)} C. \quad (21)$$

Similarly, in order to derive the equivalent capacitance of C1a (eq), the following equation can be derived:

$$\begin{cases} C\Delta V_{c1a} = kI_O T_S \\ C\Delta V_{c3a} = (k-1) I_O T_S \\ \dots \\ C\Delta V_{c2(k-1)a} = I_O T_S \end{cases} \quad (22)$$

At the same time, the following equation exists:

$$C_{1a(eq)} \Delta V' = I_O T_S \quad (23)$$

Where

$\Delta V' = \Delta V_{c1a} + \Delta V_{c3a} + \dots \Delta V_{c(2k-1)a}$. Therefore, the expression of C1a (eq) is obtained

International Journal for Innovative Engineering and Management Research
A Peer Revieved Open Access International Journal
www.ijiemr.org

$$C_{1a(eq)} = \frac{2}{(k+1)k}C \tag{24}$$

Because of the symmetry, the equivalent capacitance C1b (eq) and C2b (eq) is given as following:

$$C_{1b(eq)} = \frac{2}{(k+1)k}C \tag{25}$$

$$C_{2b(eq)} = \frac{2D'}{k(k-1+2D')}C \tag{26}$$

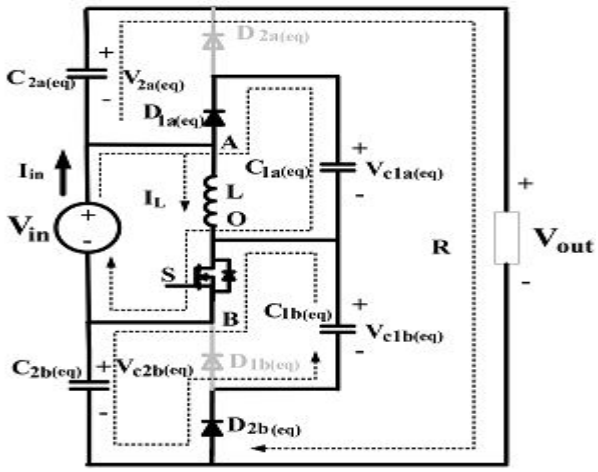

(a)

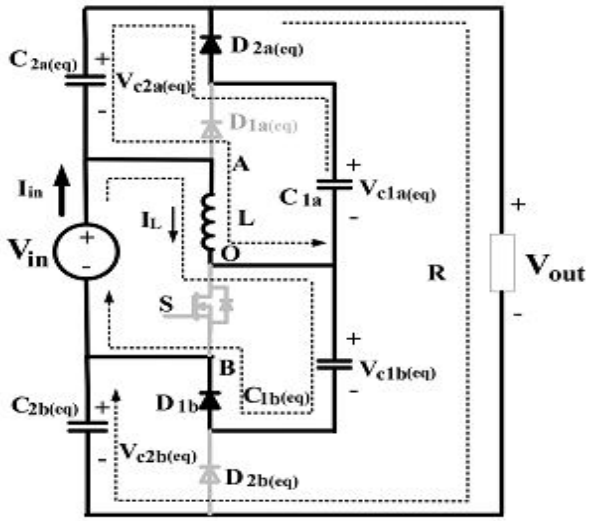

(b)

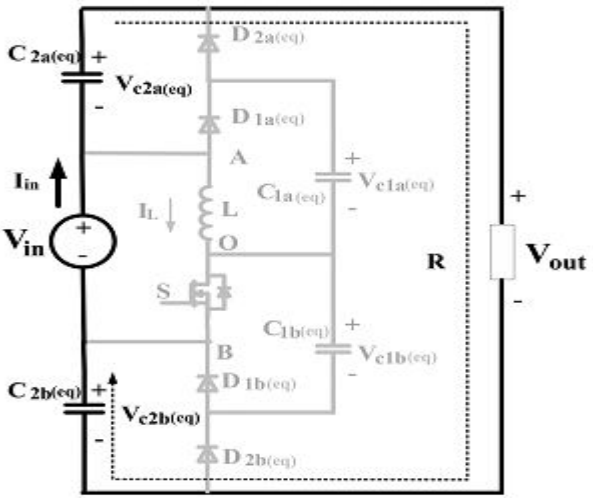

(c)

Fig.5.Three operation states, (a) State 1[0, DTs]. (b) State 2[DTs, (D+D1) Ts]. (c) State 3[(D+D1) Ts, Ts]

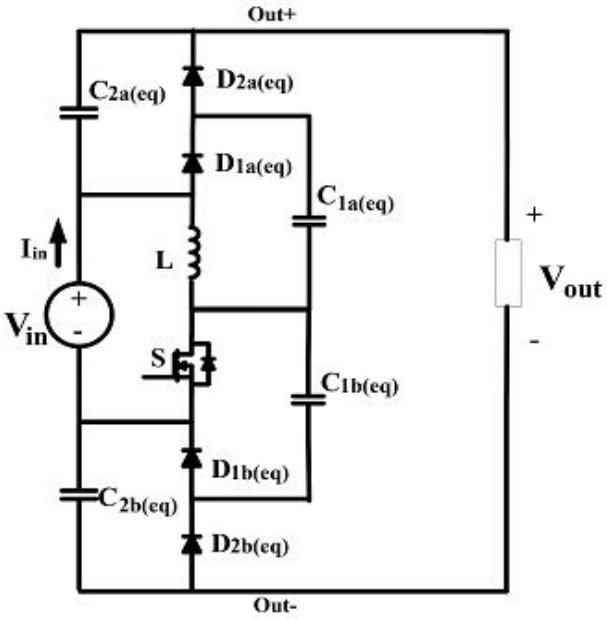

Fig.6. Equivalent even-order HBC

The derivation of voltage and equivalent value of the equivalent flying capacitors can facilitate the output voltage calculation and ripple estimation.

C. Operation Principle of General Basic HBC

Based on the simplification method discussed in previous section, the general even-

International Journal for Innovative Engineering and Management Research
A Peer Revieved Open Access International Journal
www.ijiemr.org

order HBC in Fig.1 (b) can be simplified to an equivalent HBC circuit, shown as Fig.5. Careful examination of the topology indicates that the two "boost" like sub circuits are intertwined through the operation of the active switch S. The total output voltage of HBC is the sum of the output voltage of two boost sub circuits plus the input voltage.

1) State 1[0, DTs]: In Fig. 5(a), switch S is turned on and diodes D1a (eq), D2b (eq) conduct while diodes D2a (eq) and D1b (eq) are reversely biased. The inductor L is charged by the input source. Meanwhile, capacitor C1a (eq) is charged by input source and capacitor C2b (eq) is charged by capacitor C2b (eq). At this interval, the following equations can be derived based on the inductive switching core analysis:

$$V_{AO+} = V_{in} \quad (27)$$

$$V_{OB-} = 0 \quad (28)$$

2) State 2[DTs,(D+D1)Ts]: As illustrated in Fig.5(b), when S is turned off, the inductor current will free wheel through diodes D2a (eq) and D1b (eq) .The inductor is shared by two charging boost loops. In the top loop, capacitor C1a (eq) is releasing energy to capacitor C2a (eq) and load at the same time. In the bottom loop, input source charges capacitor C1b (eq) through the inductor L. During this time interval, voltage generated at AO and OB is expressed as following based on inductor balance principal:

$$V_{AO+} = -V_{in}\frac{D}{D_1} \quad (29)$$

$$V_{OB+} = \frac{V_{in}(D+D_1)}{D_1} \quad (30)$$

3) State 3[(D+D1) Ts, Ts]: Under certain conditions, the circuit will work under DCM operation mode, thus the third state in Fig.5(c) appeals. At this state, the switch S is kept off. The inductor current has dropped to zero and all the diodes are blocked. The capacitor C2a (eq) and C2a (eq) are in series with input source to power the load. During this time interval, voltage generated at port AO is zero while at OB is Vin

$$V_{c2b(eq)} = k\frac{V_{in}}{D'} \quad (31)$$

$$V_{c2a(eq)} = k\frac{V_{in}}{D'} \quad (32)$$

$$\frac{V_{out}}{V_{in}} = 1 + 2k\frac{1}{D'} \quad (33)$$

$$V_{out} = V_{in} + 2kV_{in}\frac{D+D_1}{D_1} \quad (34)$$

$$I_L = I_{D2a(eq)} + I_{D1b(eq)} \quad (35)$$

$$\overline{I_{D2a(eq)}} = \overline{I_{D1b(eq)}} = I_O \quad (36)$$

As current waveforms of ID2a (eq) and ID1b (eq) should both have triangle shape, they will share same peak current value, which is half of the inductor peak current. Therefore

$$I_{D2a(eq)p-p} = I_{D1b(eq)p-p} = \frac{1}{2}\frac{V_{in}}{L}DT_S \quad (37)$$

The average current of ID2a (eq) in a switching period is I_O, thus

$$\frac{1}{2}D_1T_S\frac{1}{2}\frac{V_{in}}{L}DT_S\frac{1}{T_S} = I_O \quad (38)$$

$$D_1 = \frac{4I_OL}{V_{in}T_SD} \quad (39)$$

Substituting (37) to (32), the following equation can be derived:

$$V_{out} = V_{in} + 2k\left(V_{in} + \frac{V_{in}^2D^2T_S}{4I_OL}\right) \quad (40)$$

Solving the (38) gives the voltage gain in DCM mode

$$\frac{V_{out}}{V_{in}} = \frac{2k+1+\sqrt{(2k+1)^2+k\frac{2D^2T_SR}{L}}}{2} \quad (41)$$

In order to derive boundary condition for CCM and DCM mode, the average power balance is used

International Journal for Innovative Engineering and Management Research
A Peer Revieved Open Access International Journal
www.ijiemr.org

$$V_{\text{in}}(\overline{I_L} + \overline{I_{D1a(eq)}}) = V_{\text{out}} I_O \quad (42)$$

Where

$$\overline{I_{D1a(eq)}} = I_O = \frac{V_{\text{out}}}{R}$$

Thus, the average current of I_L under CCM condition is

$$\overline{I_L} = \frac{2k}{D'} \frac{V_{\text{out}}}{R} \quad (43)$$

The current ripple of inductor is

$$\Delta i_L = \frac{V_{\text{in}}}{2L} D T_S \quad (44)$$

Therefore, the CCM condition is

$$\frac{2k}{D'} \frac{V_{\text{out}}}{R} > \frac{V_{\text{in}}}{2L} D T_S \quad (45)$$

The criteria can be rearranged as

$$\frac{2L}{R T_S} > \frac{D D'^2}{2k(D' + 2k)} = K_{\text{crit}}(D) \quad (46)$$

III. INDUCTION MOTOR

An asynchronous motor type of an induction motor is an AC electric motor in which the electric current in the rotor needed to produce torque is obtained by electromagnetic induction from the magnetic field of the stator winding. An induction motor can therefore be made without electrical connections to the rotor as are found in universal, DC and synchronous motors. An asynchronous motor's rotor can be either wound type or squirrel-cage type.

Three-phase squirrel-cage asynchronous motors are widely used in industrial drives because they are rugged, reliable and economical. Single-phase induction motors are used extensively for smaller loads, such as household appliances like fans. Although traditionally used in fixed-speed service, induction motors are increasingly being used with variable-frequency drives (VFDs) in variable-speed service. VFDs offer especially important energy savings opportunities for existing and prospective induction motors in variable-torque centrifugal fan, pump and compressor load applications. Squirrel cage induction motors are very widely used in both fixed-speed and variable-frequency drive (VFD) applications. Variable voltage and variable frequency drives are also used in variable-speed service.

In both induction and synchronous motors, the AC power supplied to the motor's stator creates a magnetic field that rotates in time with the AC oscillations. Whereas a synchronous motor's rotor turns at the same rate as the stator field, an induction motor's rotor rotates at a slower speed than the stator field. The induction motor stator's magnetic field is therefore changing or rotating relative to the rotor. This induces an opposing current in the induction motor's rotor, in effect the motor's secondary winding, when the latter is short-circuited or closed through external impedance. The rotating magnetic flux induces currents in the windings of the rotor; in a manner similar to currents induced in a transformer's secondary winding(s). The currents in the rotor windings in turn create magnetic fields in the rotor that react against the stator field. Due to Lenz's Law, the direction of the magnetic field created will be such as to oppose the change in current through the rotor windings. The cause of induced current in the rotor windings is the rotating stator magnetic field, so to oppose the change in rotor-winding currents the rotor will start to rotate in the direction of the rotating stator magnetic field. The difference, or "slip," between actual and synchronous speed varies from about 0.5 to 5.0% for standard Design B torque curve induction motors. The induction machine's essential character is that it is created solely by induction instead of being separately excited as in synchronous or DC machines or being self-magnetized as in permanent magnet motors.

For rotor currents to be induced the speed of the physical rotor must be lower than that of the stator's rotating magnetic field (n_s); otherwise the magnetic field would not be

International Journal for Innovative Engineering and Management Research
A Peer Revieved Open Access International Journal
www.ijiemr.org

moving relative to the rotor conductors and no currents would be induced. As the speed of the rotor drops below synchronous speed, the rotation rate of the magnetic field in the rotor increases, inducing more current in the windings and creating more torque. The ratio between the rotation rate of the magnetic field induced in the rotor and the rotation rate of the stator's rotating field is called slip. Under load, the speed drops and the slip increases enough to create sufficient torque to turn the load.

Synchronous Speed:

The rotational speed of the rotating magnetic field is called as synchronous speed.

$$Ns = \frac{120 \times f}{P} \quad (RPM) \qquad (47)$$

Where,

f = frequency of the supply

P = number of poles

Slip:

Rotor tries to catch up the synchronous speed of the stator field, and hence it rotates. But in practice, rotor never succeeds in catching up. If rotor catches up the stator speed, there won't be any relative speed between the stator flux and the rotor, hence no induced rotor current and no torque production to maintain the rotation. However, this won't stop the motor, the rotor will slow down due to lost of torque, and the torque will again be exerted due to relative speed. That is why the rotor rotates at speed which is always less the synchronous speed.

The difference between the synchronous speed (Ns) and actual speed (N) of the rotor is called as slip.

$$\%\ slip \quad s = \frac{Ns - N}{Ns} \times 100 \qquad (48)$$

IV. MATLAB/SIMULINK RESULTS

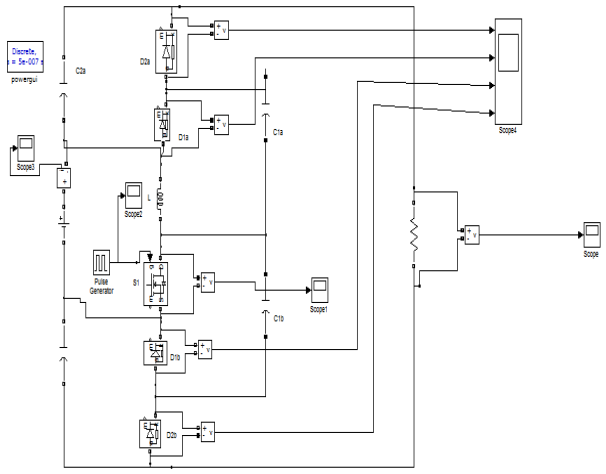

Fig.7 MATLAB/SIMULINK circuit for even-order Hybrid Boost Converter (HBC)

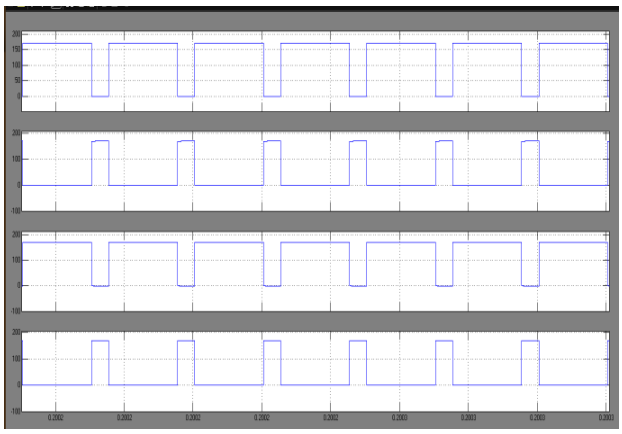

Fig.8 Diode voltage (1a, 2a, 1b and 2b)

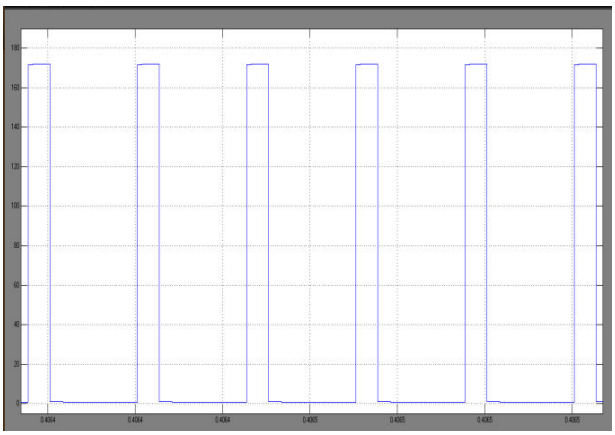

Fig.9 Switch voltage

International Journal for Innovative Engineering and Management Research
A Peer Revieved Open Access International Journal
www.ijiemr.org

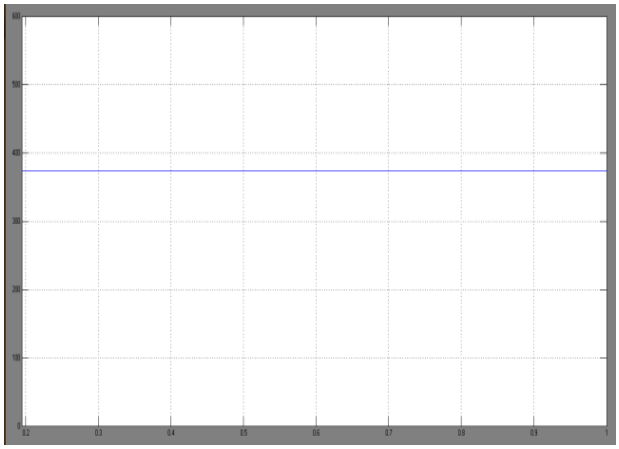

Fig.10 Output voltage

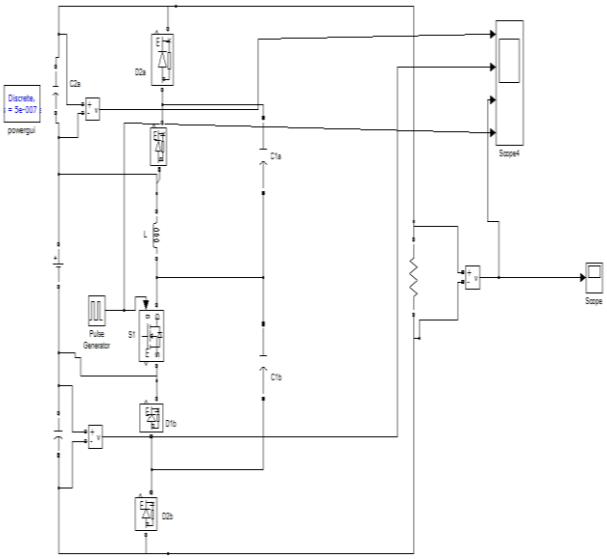

Fig.11 MATLAB/SIMULINK circuit for even-order Hybrid Boost Converter (HBC)

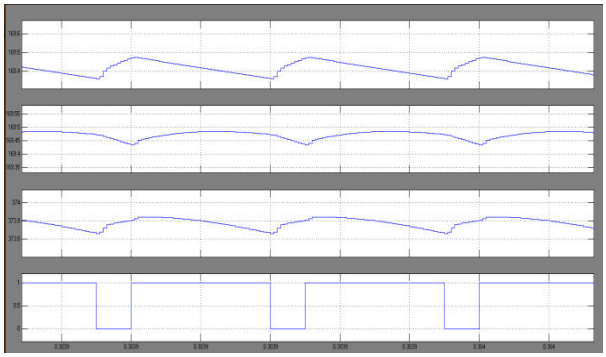

Fig.12 Capacitor voltages (Vc2a, Vc2b), Switch voltage and output voltage

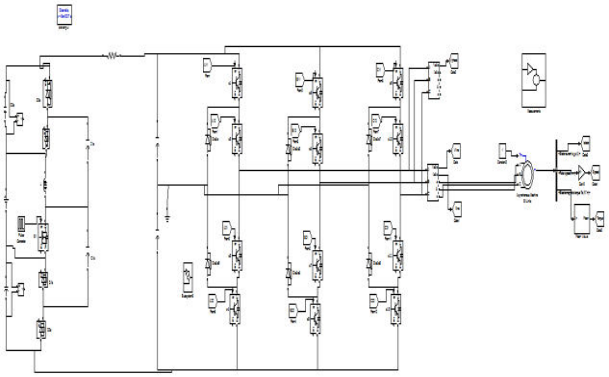

Fig.13MATLAB/SIMULINK circuit for even-order Hybrid Boost Converter (HBC) with Induction motor drive

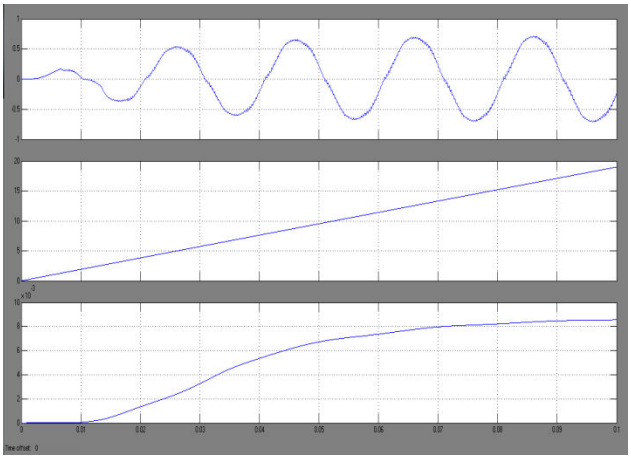

Fig.14 Stator current ,Speed and Electromagnetic torque

V. CONCLUSION

The system descried here is a PV system employing a hybrid boost converter and motor. The boost converter is used to step up the low input voltage produced by PV array. The proposed scheme is thus successfully used to drive an induction motor. The advantage of the proposed control technique is controlling the Induction motor at variable speed conditions with high response, high efficiency, and high robustness and minimum steady state error. The Simulation results on MATLAB/Simulink are presented.

REFERENCES

[1] Mr. Lili Kumar Uttarala, Dr. J. Viswanatha Rao, Mr. Kranthi Kumar. Vanukuru and Mrs.

Battula Asha Kiran, "Res Fed High Gain Dc-Dc Converter with Closed Loop Control for Induction Motor Drive," International conference on Signal Processing, Communication, Power and Embedded System (SCOPES)-2016.

[2] N. Vazquez, L. Estrada, C. Hernandez, and E. Rodriguez, "The tapped inductor boost converter," in Proc. IEEE Int. Symp. Ind. Electron., Jun. 2007, pp. 538–543.

[3] W. Chen, A. Q. Huang, C. Li, G. Wang, and W. Gu, "Analysis and comparison of medium voltage high power DC/DC converters for offshore wind energy systems,"IEEE Trans. Power Electron., vol. 28, no. 4, pp. 2014–2023, Apr. 2013.

[4] J. A. Starzyk, "A DC-DC charge pump design based on voltage doublers," IEEE Trans. Circuits Syst. I Fundam. Theory Appl., vol. 48, no. 3, pp. 350–359, Mar. 2001.

[5] F. L. Luo and H. Ye, "Positive output multiple-lift push–pull switched capacitor luo-converters," IEEE Trans. Ind. Electron., vol. 51, no. 3, pp. 594–602, Jun. 2004.

[6] R. Wai, C. Lin, R. Duan, and Y. Chang, "High-efficiency DC-DC converter with high voltage gain and reduced switch stress," IEEE Trans. Ind. Electron., vol. 54, no. 1, pp. 354–364, Feb. 2007.

[7] A. Lamantia, P. G. Maranesi, and L. Radrizzani, "Small-signal model of the Cockcroft-Walton voltage multiplier," IEEE Trans. Power Electron., vol. 9, no. 1, pp. 18–25, Jan. 1994.

[8] J. Lee, T. Liang, and J. Chen, "Isolated coupled-inductor-integrated DC–DC converter with non dissipative snubber for solar energy applications," IEEE Trans. Ind. Electron., vol. 61, no. 7, pp. 3337–3348, Jul. 2014.

[9] M. Delshad and H. Farzanehfard, "High step-up zero-voltage switching current-fed isolated pulse width modulation DC–DC converter," IET Power Electron., vol. 4, no. 3, pp. 316–322, Mar. 2011.

[10] P. Lin and L. Chua, "Topological generation and analysis of voltage multiplier circuits," IEEE Trans. Circuits Syst., vol. 24, no. 10, pp. 517–530, Oct. 1977.

[11] X. Hu and C. Gong, "A high voltage gain DC–DC converter integrating coupled-inductor and diode–capacitor techniques," IEEE Trans. Power Electron., vol. 29, no. 2, pp. 789–800, Feb. 2014.

[12] K.-C. Tseng, C.-C.Huang, and W.-Y. Shih, "A high step-up converter with a voltage multiplier module for a photovoltaic system,"IEEE Trans. Power Electron., vol. 28, no. 6, pp. 3047–3057, Jun. 2013.

[13] W. Li, W. Li, X. Xiang, Y. Hu, and X. He, "High step-up interleaved converter with built-in transformer voltage multiplier cells for sustainable energy applications,"IEEE Trans. Power Electron., vol. 29, no. 6, pp. 2829–2836, Jun. 2014.